

Contents lists available at ScienceDirect

Physics Letters B

www.elsevier.com/locate/physletb

Explaining the CMS dilepton mass endpoint in the NMSSM

Bhaskar Dutta^a, Yu Gao^{a,*}, Tathagata Ghosh^a, Teruki Kamon^{a,b}, Nikolay Kolev^c^a Department of Physics and Astronomy, Mitchell Institute for Fundamental Physics and Astronomy, Texas A&M University, College Station, TX 77843-4242, USA^b Department of Physics, Kyungpook National University, Daegu 702-701, South Korea^c Department of Physics, University of Regina, SK S4S 0A2, Canada

ARTICLE INFO

Article history:

Received 28 June 2015

Received in revised form 29 July 2015

Accepted 6 August 2015

Available online 10 August 2015

Editor: J. Hisano

ABSTRACT

NMSSM scenarios are investigated to explain an excess in the opposite-sign dilepton mass distribution in events with dilepton, jets and missing transverse energy reported by the CMS experiment. We show that the NMSSM scenarios can possess unique features to explain this excess, and can be distinguished from the MSSM scenarios in the ongoing LHC runs as well as direct detection experiments.

© 2015 Published by Elsevier B.V. This is an open access article under the CC BY license (<http://creativecommons.org/licenses/by/4.0/>). Funded by SCOAP³.

1. Introduction

Recently, the CMS collaboration reported of an excess of lepton pairs [1] with energy below the Z mass in a final state of $l^+l^-jj + \cancel{E}_T$ at a level of approximately 2σ . Although they do not specify these jets to be b -tagged, their physics interpretation is based on cascade decays from the sbottom pair production in the context of the Minimal Supersymmetric Standard Model (MSSM). The ATLAS Collaboration, however, has not observed a similar excess [2]. It would be interesting to repeat the analyses in Run II of the LHC.

In this paper, the CMS excess is explained in a framework of Next-to MSSM (NMSSM). NMSSM possesses unique features, compared with other interpretations such as MSSM [1,3–5], a lepto-quark scenario [6] and superstring inspired models [7], and can be distinguished from them.

Two same-flavor, opposite-sign leptons can be produced from a cascade decay that has particles decay into leptons in the intermediate state during the process. Such lepton partners and heavier states, which give rise to the cascades, are readily available in supersymmetric models. The sbottom pair production and its cascade decays into the next to lightest neutralino which subsequently decays into two leptons and the lightest neutralino via an intermediate slepton state is a very interesting option to explain the excess. Two b jets are also produced along with $l^+l^- + \cancel{E}_T$ in the final states. The existence of two b jets in the signal provides an interesting prediction arising from this scenario which will be checked in Run II. Prior to this new result, $l^+l^-jj + \cancel{E}_T$ was considered as a possible final state from the stop decay [8]. Since

we have $\tilde{t} \rightarrow t + \tilde{\chi}_2^0$, we expect lepton(s) from top decay in addition to $\tilde{\chi}_2^0 \rightarrow l^+l^- \tilde{\chi}_1^0$. This does not support the CMS edge paper. In this paper we focus on a well motivated Next-to Minimal Supersymmetric Standard Model [9] (NMSSM), which introduces an additional singlet superfield into the MSSM. The observed Higgs mass at the LHC [10] can be accommodated naturally if the coupling λ between the singlet and the supersymmetric Higgs fields is large and this new term also provides a solution to the μ problem of the MSSM (see [11] and references therein). Recently, signals of such a scenario at the LHC were investigated and possible ways to distinguish from the MSSM were also discussed [12].

The singlet superfield in the NMSSM gives rise to a new neutralino (singlino) to the gaugino sector, besides other modification on the MSSM particle spectrum. This paper investigates the effect of the singlino that creates more freedom to realize the aforementioned cascade decays of sbottom, which alleviates a relatively tight requirement on the MSSM neutralino mixings. Further, since the neutralino sector is modified, the NMSSM explanation will be associated with distinguishable predictions at the LHC.

The cascade process to explain the endpoint in the context of the NMSSM is discussed in Section 2. A collider analysis is carried out in Section 3 that examines the NMSSM's explanation of the CMS dilepton excess. We discuss our results and the differences between our NMSSM benchmarks from the MSSM in Section 4.

2. Squark-neutralino cascades

In supersymmetric models, the CMS excess in the relatively low mass ‘endpoint’ in opposite sign dileptons can rise from the decays of one or more heavier neutralinos. A leading example is the second lightest neutralino that can decay via a two-step process,

$$\tilde{\chi}_2^0 \rightarrow l^+\tilde{l}^-, \tilde{l}^- \rightarrow l^- \tilde{\chi}_1^0, \quad (1)$$

* Corresponding author.

E-mail address: yugao@physics.tamu.edu (Y. Gao).

Table 1

The NMSSM benchmark points that yield same-flavor opposite-sign lepton pairs in sbottom cascade decays. The mass spectrum is evaluated using NMSSMTools [17] and its values are given in GeV. l denotes both left and right sleptons of the first two lepton flavors.

| | M_1 | M_2 | $\tan\beta$ | λ | κ | μ_{eff} | $M_{\tilde{\chi}_1^0}$ | $M_{\tilde{\chi}_2^0}$ | $M_{\tilde{b}_1}$ | $M_{\tilde{\chi}_1^\pm}$ | M_t |
|---|-------|-------|-------------|-----------|----------|--------------------|------------------------|------------------------|-------------------|--------------------------|-------|
| A | 500 | 315 | 3.1 | 0.7 | 0.143 | 600 | 250 | 320 | 373 | 315 | 285 |
| B | 248 | 800 | 15 | 0.5 | 0.265 | 330 | 230 | 300 | 357 | 333 | 265 |
| C | 310 | 800 | 10 | 0.6 | 0.14 | 500 | 229 | 305 | 357 | 500 | 850 |

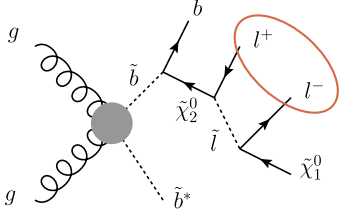


Fig. 1. Pair production of sbottoms and one of its cascade decay chains can give rise to a signal of lepton pairs with energy below the neutralino mass difference. The other sbottom in the diagram presumably decays directly to $\tilde{\chi}_1^0 b$.

which yields a pair of leptons of the same flavor, whose total energy and invariant mass distribution are both capped by the mass difference $M_{\tilde{\chi}_2^0} - M_{\tilde{\chi}_1^0}$. Here \tilde{l} denotes both the left and right sleptons in the first two lepton flavors.

Thus a neutralino spectrum with $M_{\tilde{\chi}_2^0} \sim M_{\tilde{\chi}_1^0} + 70$ GeV can lead to such a dilepton excess if the slepton masses lie between the two neutralino masses and if the second neutralino can be produced at adequate rates.

The QCD-dominated production of sbottom¹ can lead to the correct pair-production rates for the CMS experiment. A mostly right-handed sbottom (denoted by \tilde{b}_1 here) can be a perfect candidate [1] that decays into the required neutralinos. The Feynman diagram for the production process is illustrated in Fig. 1. The sbottom is preferably right-handed as it does not require a left-handed stop to be equally light in mass. Moreover, the CMS non-observation of more than two leptons in this channel puts a constraint on the decay of such a sbottom, i.e., the branching fraction, $\text{BF}(\tilde{b}_1 \rightarrow \tilde{\chi}_1^0 b)$, should dominate over $\text{BF}(\tilde{b}_1 \rightarrow \tilde{\chi}_2^0 b)$ unless the latter produces many lepton pairs in a final state from the pair of sbottoms. This requirement, however, may force certain relations among the neutralino mixings.

In the MSSM, a sbottom can decay into a b quark and a neutralino via either the $U(1)_Y$ gauge coupling or the Yukawa coupling. The $U(1)_Y$ gauge coupling depends on the Bino (\tilde{B}) component of the daughter neutralino, while the Yukawa coupling depends on the down-type Higgsino (\tilde{H}_d) component and the size of the coupling y_d . If the model assumes 100% of the relic dark matter density is made out of the LSP, the MSSM's LSP needs to be dominantly Bino to avoid increasingly severe experimental constraints (from indirect [13,14] and direct [15] detections). However, the Bino content of the neutralinos would strongly affect the sbottom decay rate into them. A mass difference $M_{\tilde{\chi}_2^0} - M_{\tilde{\chi}_1^0} \approx 70$ GeV would leave too little Bino content in $\tilde{\chi}_2^0$ for the $\tilde{b}_1 \rightarrow \tilde{\chi}_2^0 b$ decay to occur (by a few orders of magnitude when only the gauge couplings contribute, i.e., for smaller $\tan\beta$). To solve this problem, as in Ref. [3], $\tilde{\chi}_2^0$ needs a large mixing of the Higgsinos (and also a large $\tan\beta$) to boost the branching fraction of the $\tilde{b}_1 \rightarrow \tilde{\chi}_2^0 b$ decay via the enhanced Yukawa couplings. This scenario, however,

also requires a low mass Higgsino type lightest chargino which is detectable by a direct production in the ongoing run.

In the NMSSM, however, the option of a singlino LSP opens up larger parameter space with an alternative neutralino mixing scenarios to realize sbottom decays into both $\tilde{\chi}_1^0$ and $\tilde{\chi}_2^0$ in a suitable way (i.e., without suffering from the direct and indirect dark matter detection constraints) which differs from the MSSM, e.g., we may not need any low mass chargino by having $\tilde{\chi}_1^0$ and $\tilde{\chi}_2^0$ to be made out of mostly singlino and Bino. Consequently, the collider signals arising from the direct production of neutralinos, charginos will be helpful to discern the MSSM from the NMSSM at the LHC.

(A) We can satisfy the CMS excess for mostly singlino LSP and a heavy Bino. The components of \tilde{B} in both $\tilde{\chi}_1^0$, $\tilde{\chi}_2^0$ are small but comparable in magnitude for heavier \tilde{B} . This allows a small $\tan\beta$ scheme where both $\tilde{b}_1 \rightarrow \tilde{\chi}_1^0 b$, $\tilde{\chi}_2^0 b$ decays occur via the $U(1)_Y$ coupling, while the down-type Yukawa contribution to the decays is small.

The next to lightest supersymmetry particle (NLSP) can be wino and/or Higgsino. A wino-NLSP case is shown in Table 1. In comparison, when the NLSP is mainly Higgsino, $\tilde{\chi}_3^0$ would be relatively light and the sbottom may decay into two NLSPs. However, the Higgsino-NLSP case tends to allow the LSP to have a larger Higgsino mixing which faces constraint from the direct detection result unless we chose the correct sign of gaugino, Higgsino mass parameters to cancel the Higgs contribution in the direct detection amplitude [16].

(B) We can satisfy the CMS excess for mostly Bino type $\tilde{\chi}_1^0$, where $\tilde{\chi}_2^0$ is mostly singlino and $\tilde{\chi}_{3,4}^0$ consist of mostly Higgsinos and Wino. Just like the MSSM, a large $\tan\beta$ is required to boost the decay via down-type Yukawa coupling to the \tilde{H}_d component in $\tilde{\chi}_2^0$, which is closer in mass to the Higgsinos in comparison to the much lighter $\tilde{\chi}_1^0$. The major difference of this scenario from the MSSM is that the lightest chargino $\tilde{\chi}_1^\pm$ mass is close to $\tilde{\chi}_3^0$ rather than $\tilde{\chi}_2^0$, and consequently can be heavier than that of the MSSM. This allows a wider mass range of the sbottom after satisfying $M_{\tilde{b}_1} - M_{\tilde{\chi}_1^\pm} < M_t$ so that \tilde{b}_1 does not decay into top quarks.

(C) We can also satisfy the CMS excess for a mostly singlino type $\tilde{\chi}_1^0$ where $\tilde{\chi}_2^0$ is mostly Bino. Since $\tilde{\chi}_2^0$ is mostly Bino, $\text{BF}(\tilde{b}_1 \rightarrow \tilde{\chi}_2^0 b)$ is large and yields a large number of final state leptons via sleptons situated in between the two neutralinos which may not be a suitable option. A virtual slepton mediated three-body decay $\{\tilde{\chi}_2^0 \rightarrow \tilde{l}^* l^+, \tilde{l}^* \rightarrow l^- \tilde{\chi}_1^0\}$, however, can give the correct $2l + \cancel{E}_T$ rate. This parameter space is represented by point C which shows that the slepton masses are much higher than the $\tilde{\chi}_{1,2}^0$ mass range, e.g., the slepton masses are almost at TeV scale for point C. It is interesting to note that even if we imagine a scenario where the slepton masses are very close to either $\tilde{\chi}_2^0$ or $\tilde{\chi}_1^0$, and only one of the leptons from each sbottom cascade is visible, the invariant mass of the two leptons from different cascades can easily be more than 70 GeV and contradicts with observation. Also, unlike the Points A and B, the two leptons do not have fixed energies in the three body decay and can cause a spectral difference in the invariant mass distribution, as will be shown in the next section.

¹ The dilepton mass endpoint can also be produced from the decay of a light stop, but when stop is pair produced we also expect to see multilepton final state and the non-observation of more than two leptons along with 2 jet and \cancel{E}_T makes this scenario not preferred.

Table 2

\tilde{b}_1 decay branching fractions and the dilepton selection efficiencies for the benchmark points. ϵ_{ll} is given in Eq. (3). $\text{BF}_{\tilde{\chi}_2^0 \rightarrow \tilde{l}\tilde{l}}$ for point C in column 4 should read as $\text{BF}_{\tilde{\chi}_2^0 \rightarrow \tilde{l}\tilde{l}^*}$.

| | $\text{BF}_{\tilde{b}_1 \rightarrow \tilde{\chi}_1^0 b}$ | $\text{BF}_{\tilde{b}_1 \rightarrow \tilde{\chi}_2^0 b}$ | $\text{BF}_{\tilde{\chi}_2^0 \rightarrow \tilde{l}\tilde{l}}$ | ϵ_{ll} |
|---|--|--|---|-----------------|
| A | 69% | 31% | 25% | 38% |
| B | 90% | 10% | 57% | 38% |
| C | 10% | 89% | 11% | 26% |

Table 3

The selection efficiencies for the $l^+l^-jj + \cancel{E}_T$ signal at benchmark points A, B and C.

| Event selection | Relative efficiency | | |
|---|---------------------|-------|-------|
| | A | B | C |
| σ_{NLO} (fb) | 660 | 854 | 854 |
| $N_j \geq 2(3) + \cancel{E}_T > 150(100)$ GeV | 32% | 37% | 25% |
| Two isolated OSSF leptons | 3.2% | 2.3% | 3.2% |
| Dileptons in the central region | 85% | 85% | 84% |
| Overall acceptance | 0.85% | 0.72% | 0.66% |
| Number of events at 20 fb^{-1} | 112 | 124 | 112 |

3. Collider signal

Here we discuss the dilepton yield from the NMSSM benchmark points at the 8 TeV LHC. At each point, a mass gap is kept at 70 GeV between the two lightest neutralinos that limits the energy of the lepton pair. $\tilde{\chi}_3^0$ is above \tilde{b}_1 and all sfermions other than \tilde{l} and \tilde{b}_1 have multi-TeV masses and decouple from our study.² The lightest chargino $\tilde{\chi}_1^\pm$ mass is not lighter than $M_{\tilde{b}_1} - M_t$, which can be used as one aspect that the NMSSM spectrum differs from the MSSM's. The \tilde{b}_1 is mostly right-handed and its decay BF's are listed in Table 2, together with the BF of $\tilde{\chi}_2^0$'s decay to \tilde{l} and the lepton reconstruction efficiency. The $\text{BF}(\tilde{l} \rightarrow l\tilde{\chi}_1^0)$ decay is 100% for all of our benchmark points, since in all these cases the LSP is either a singlino or bino.

We generate inclusive sbottom pair production events with 0–2 associated jets at 8 TeV in MadGraph5 v2.2.2 [18] with CTEQ6.6 [19] parton distribution functions. Pythia v6.426 [20] is used for showering and hadronization and PGS4 [21] is used for detector simulation in which the electron and muon detection efficiencies are assumed to be 92% and 98%, respectively. To avoid double-counting of jets the MLM jet matching scheme [22] is implemented. We provide the decay tables for supersymmetry particles generated by NMSMTools [23] to Pythia v6.426 for all the benchmark points and subsequently isotropic phase space two body (Point A and B) three body (Point C) decay of $\tilde{\chi}_2^0$ is carried out by Pythia v6.426, without spin-correlations.

The LO production cross section $\sigma_{\text{LO}} \approx 500 \text{ fb}$ for sbottom with approximately 360 GeV mass. This is scaled up by a K-factor of 1.7 to the NLO value that is obtained from the package Prospino [24]. The dilepton signal rate is then,

$$(20 \text{ fb}^{-1}) \cdot \sigma_{\text{NLO}} \cdot A_{\text{eff}}, \quad (2)$$

where A_{eff} denotes the total event selection acceptance. The selection criteria for the jet and lepton objects are as follows: $p_T(\text{jet}) > 40 \text{ GeV}$ with $|\eta| < 3$, $p_T(\text{lepton}) > 20 \text{ GeV}$ with $|\eta| < 2.4$, excluding $1.4 < |\eta| < 1.6$; the central region is defined as $|\eta| < 1.4$.

The selection efficiency flows for points A, B and C are shown in Table 3. Overall acceptances are similar for A and B. The first cut

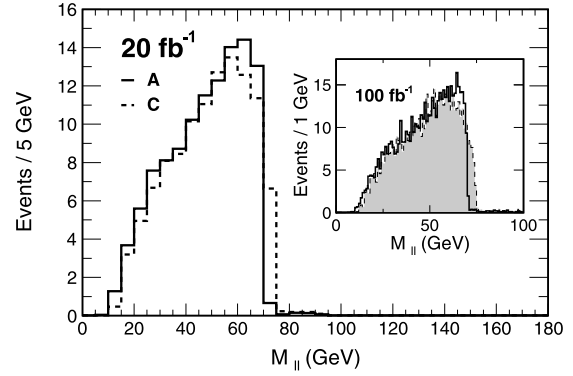


Fig. 2. Invariant mass distribution of the opposite sign same flavor dileptons after implementing all selection cuts. The distributions are based on MC sample of 1000 fb^{-1} integrated luminosity but normalized to 20 and 100 fb^{-1} integrated luminosities.

is the “OR” cut from the CMS analysis [1]: it selects events with at least 2 jets and $\cancel{E}_T > 150 \text{ GeV}$, or at least 3 jets and $\cancel{E}_T > 100 \text{ GeV}$. We find that point C shows lower efficiency at this stage compared to points A and B. This is due to the fact that \tilde{b}_1 has a larger branching ratio into $\tilde{b}_1 \rightarrow b + \tilde{\chi}_1^0$ for points A and B where $\tilde{\chi}_1^0$ is mostly Bino compared to the point C where $\tilde{\chi}_1^0$ is mostly singlino. A large mass gap ($\sim 120 \text{ GeV}$) between \tilde{b}_1 and $\tilde{\chi}_1^0$ at the points A and B leads to higher p_T jets. In contrast, at point C, a smaller mass gap ($\sim 50 \text{ GeV}$) between \tilde{b}_1 and $\tilde{\chi}_2^0$ produces lower p_T jets that cause a lower efficiency at the $p_T(\text{jet}) > 40 \text{ GeV}$ cut. As a compensation, \tilde{b}_1 at point C has a larger decay branching into $b + \tilde{\chi}_2^0$. The fraction of isolated leptons is a combination of the $\tilde{b}, \tilde{\chi}_2^0$ decay branching fractions and dilepton selection efficiency ϵ_{ll} ,

$$2 \cdot x(1-x) \epsilon_{ll}, \quad (3)$$

$$x \equiv \text{BF}(\tilde{b}_1 \rightarrow \tilde{\chi}_2^0 b) \text{BF}(\tilde{\chi}_2^0 \rightarrow \tilde{l}\tilde{l}).$$

ϵ_{ll} is a fraction of events with at least two reconstructed OSSF leptons passing the lepton selection criteria out of the events with two OSSF leptons from the $\tilde{\chi}_2^0$ decays. In principle, ϵ_{ll} can vary with the lepton energy that is determined by the mass difference between the sleptons and neutralinos. At points A and B, when $M_{\tilde{l}} \sim (M_{\tilde{\chi}_1^0} + M_{\tilde{\chi}_2^0})/2$ with both leptons at $E_l = 35 \text{ GeV}$, we get maximal acceptance of $\epsilon_{ll} \approx 38\%$. At point C the leptons arise from a three body decay and the energy partition becomes uneven, and the acceptance can suffer if one of the leptons is too soft. The lepton pairs are further required to be in the central region with pseudorapidity $|\eta| < 1.4$, and finally the overall acceptance gives the accumulated selection efficiency.

A dilepton signal of around 120 events are obtained for all the three benchmark points. The dilepton mass distributions for points A and B are similar, and they both show a clear dilepton invariant mass endpoint at $M_{\tilde{\chi}_2^0} - M_{\tilde{\chi}_1^0}$ as each of two leptons has a fixed 35 GeV energy, where the invariant mass of the dilepton maximizes. The endpoint for point C is less pronounced due to the possible unequal energy between the two leptons in the three body decay of $\tilde{\chi}_2^0$. In Fig. 2, we show the distributions for points A and C. The distribution for point B is identical to that of point A and is not shown. As the lepton energy is well measured at the LHC, it is possible to discriminate point C from other points by performing shape analysis with finer binning and higher integrated luminosity, as is shown in the inset. The statistical fluctuations in Fig. 2 corresponds to a MC sample equivalent to 1000 fb^{-1} integrated luminosity. All three benchmark points have less than 4% multi-lepton final states compared to the dilepton final states as shown

² We remain agnostic about the exact mass of other heavy squarks and ignore the small change in the NLO \tilde{b} production cross-section due to variation of them.

Table 4Number of $3l$ and $4ljj + \cancel{E}_T$ events at benchmark points A, B and C.

| Number of multilepton events at 20 fb^{-1} | A | B | C |
|--|------|------|------|
| Three lepton | 2.14 | 2.10 | 4.46 |
| Four leptons | 1.10 | 0.7 | 1.52 |

in Table 4. We have chosen $p_T > 10 \text{ GeV}$ for the third and fourth lepton in the multilepton final states.

4. Discussion and conclusion

If the CMS dilepton excess persists in the ongoing runs of the LHC, we will be able to distinguish SUSY models by investigating associated signals from those models. Here we discuss how the neutralino/chargino sector would differ between the MSSM and the benchmarked NMSSM scenarios and would allow us to distinguish the models at the LHC. The NMSSM scenarios can be distinguished even if we do not assume that LSP makes 100% of the DM content.

In the case of the MSSM, the dilepton excess requires the existence of a Higgsino-type second-lightest neutralino and a chargino for masses around 300 GeV. The ongoing 14 TeV LHC run can produce these both the second lightest neutralino and the lightest chargino directly. However, if a thermal relic density is to be explained with the LSP, the direct dark matter detection cross-section can potentially be a problem due to an appreciable mixture of Bino and Higgsino in the LSP which would push us to use the negative sign of μ (the Higgsino mixing parameter).³ For a similar scenario, this problem can be ameliorated in the NMSSM for due to potential Higgs mixing into the singlet field that does not couple to nucleons. However, NMSSM can explain the excess without having Bino–Higgsino to be the lightest two neutralinos. We summarize below the distinguishable features of NMSSM at the LHC.

For point A, the NLSP can be mostly wino. In this case, it is possible to produce winos directly and the production cross-sections by Drell–Yan and vector boson fusion processes are larger by almost a factor of 4 compared to that in the Higgsino NLSP scenarios. The current bound ($\sim 300 \text{ GeV}$ [25,26]) still allows this point since the mass difference between the $\tilde{\chi}_1^\pm$, $\tilde{\chi}_2^0$ and $\tilde{\chi}_1^0$ is small and $\tilde{\chi}_2^0 \rightarrow \tilde{l}l$ decay branching is less than what is assumed by the CMS and ATLAS. The ongoing run will probe this point which does not suffer from the direct detection constraint.

For point B, more neutralino states are involved to explain the excess. In this case the Higgsinos, which constitute mostly the $\tilde{\chi}_{3,4}^0$, are lighter than winos and they can be also be produced directly at the LHC. The 350 GeV $\tilde{\chi}_3^0$ ($m_{\tilde{\chi}_4^0}$ is 410 GeV) has a 75% decay BF into $\tilde{\chi}_3^0 \rightarrow Z\tilde{\chi}_1^0$ and most of the remaining BF is into $\tilde{\tau}\tau$. The $\tilde{\chi}_1^\pm$ is at 333 GeV and has appreciable a BF into $W + \tilde{\chi}_1^0$. We have already shown that the sbottom decays mostly into $\tilde{\chi}_2^0$ and subsequently into $\tilde{\chi}_1^0$, whereas $\tilde{\chi}_{3,4}^0$ and $\tilde{\chi}_1^\pm$ decays predominantly to $\tilde{\chi}_1^0$. The direct productions of $\tilde{\chi}_2^0$ and $\tilde{\chi}_1^0$ are small since they are mostly singlino and Bino respectively. Therefore, at least four neutralinos and one chargino will be potentially discovered at the ongoing run from two different production processes and can be used in a complimentary way to check whether this model point explanation for the excess is correct. In addition, just like the Bino–Higgsino case in the MSSM, this scenario suffers from the direct detection constraints. However, flipping the sign of the gaugino and Higgsino mass parameters, can suppress the nucleon–LSP scattering.

³ The negative sign of μ introduces an accidental cancelation in the direct detection amplitude mediated by the Higgs which causes lowered direct detection crosssection.

For both points A, B and the MSSM, the mass-gap needed for these points to explain the excess is about 35 GeV. It can be difficult to probe the sleptons directly in the current runs of the LHC due to relatively small mass-gap between \tilde{l} and the LSP. Even boosting the system with additional jets does not help, since such searches lose their efficacy for a mass splitting above $\sim 25 \text{ GeV}$ [27].

In contrast, at point C, the sleptons are relatively heavy in order not to overproduce event with more than two leptons. If the sleptons are found to be a lot heavier than the NLSP, then the point C will be needed to explain the CMS excess. However, the direct slepton production can be probed up to $\sim 700 \text{ GeV}$ [14,28] at 3000 fb^{-1} of integrated luminosity. However, since $\tilde{\chi}_2^0$ and $\tilde{\chi}_1^0$ are mostly Bino and singlino respectively, the direct production cross-sections of them are very small. Further, unlike points A, B and MSSM, this point does not have any light chargino associated with the lightest neutralinos which can be probed at the LHC. Therefore, if no other lighter neutralinos and charginos are found but the endpoint in the dilepton distribution still persists, the point C will provide the explanation. This point also does not suffer from the direct detection problem. It is also possible to discriminate point C from other points by performing shape analysis on the dilepton mass distribution.

In conclusion, if the CMS excess is proved to be correct at the ongoing run of the LHC, it will be possible to find an explanation in the context of NMSSM, which is not ruled out by the direct detection experiments and with unique features in the neutralino sector compared to the MSSM. It will be feasible to establish these NMSSM scenarios by investigating the direct productions of neutralinos, charginos and sleptons.

Acknowledgements

We thank Peisi Huang for cross-checking the lepton reconstruction efficiency in the MSSM. We also thank Kuver Sinha and Keith Ulmer for discussions. B.D., T.K. and T.G. are supported by DOE Grant DE-FG02-13ER42020. Y.G. thanks the Mitchell Institute for Fundamental Physics and Astronomy for support. T.K. is also supported in part by Qatar National Research Fund under project NPRP 5-464-1-080. N.K.'s contribution was made possible by the facilities of the Shared Hierarchical Academic Research Computing Network (SHARCNET: www.sharcnet.ca) and Compute/Calcul Canada.

References

- [1] V. Khachatryan, et al., CMS Collaboration, *J. High Energy Phys.* 04 (2015) 124.
- [2] G. Aad, et al., ATLAS Collaboration, *Eur. Phys. J. C* 75 (7) (2015) 318.
- [3] P. Huang, C.E.M. Wagner, *Phys. Rev. D* 91 (2015) 015014.
- [4] P. Grothaus, S.P. Liew, K. Sakurai, arXiv:1502.05712 [hep-ph].
- [5] B. Allanach, A.R. Raklev, A. Kveltestad, arXiv:1409.3532 [hep-ph].
- [6] B. Allanach, A. Alves, F.S. Queiroz, K. Sinha, A. Strumia, arXiv:1501.03494 [hep-ph].
- [7] M. Dhuria, C. Hati, R. Rangarajan, U. Sarkar, *Phys. Rev. D* 91 (2015) 055010.
- [8] B. Dutta, T. Kamon, N. Kolev, K. Sinha, K. Wang, S. Wu, *Phys. Rev. D* 87 (2013) 095007.
- [9] J.R. Ellis, J.F. Gunion, H.E. Haber, L. Roszkowski, F. Zwirner, *Phys. Rev. D* 39 (1989) 844; M. Drees, *Int. J. Mod. Phys. A* 4 (1989) 3635; L. Durand, J.L. Lopez, *Phys. Lett. B* 217 (1989) 463.
- [10] CMS Collaboration, *J. High Energy Phys.* 06 (2013) 081, arXiv:1303.4571 [hep-ex].
- [11] U. Ellwanger, C. Hugonie, A.M. Teixeira, *Phys. Rep.* 496 (2010) 1.
- [12] B. Dutta, Y. Gao, B. Shakya, *Phys. Rev. D* 91 (2015) 035016.
- [13] J. Fan, M. Reece, *J. High Energy Phys.* 10 (2013) 124.
- [14] M.A. Ajajib, B. Dutta, T. Ghosh, I. Gogoladze, Q. Shafi, arXiv:1505.05896 [hep-ph].
- [15] M. Perelstein, B. Shakya, *J. High Energy Phys.* 10 (2011) 142; M. Perelstein, B. Shakya, *Phys. Rev. D* 88 (7) (2013) 075003.

- [16] J.L. Feng, D. Sanford, J. Cosmol. Astropart. Phys. 1105 (2011) 018;
R.L. Arnowitt, B. Dutta, Y. Santos, Nucl. Phys. B 606 (2001) 59;
J.R. Ellis, A. Ferstl, K.A. Olive, Phys. Rev. D 63 (2001) 065016.
- [17] U. Ellwanger, J.F. Gunion, C. Hugonie, J. High Energy Phys. 02 (2005) 066;
U. Ellwanger, C. Hugonie, Comput. Phys. Commun. 175 (2006) 290.
- [18] J. Alwall, M. Herquet, F. Maltoni, O. Mattelaer, T. Stelzer, Madgraph 5: going beyond, J. High Energy Phys. 06 (2011) 128;
J. Alwall, R. Frederix, S. Frixione, V. Hirschi, F. Maltoni, O. Mattelaer, H.-S. Shao, T. Stelzer, et al., J. High Energy Phys. 07 (2014) 079.
- [19] P.M. Nadolsky, H.L. Lai, Q.H. Cao, J. Huston, J. Pumplin, D. Stump, W.K. Tung, C.-P. Yuan, Phys. Rev. D 78 (2008) 013004.
- [20] T. Sjostrand, S. Mrenna, P. Skands, Pythia 6.4 physics and manual, J. High Energy Phys. 05 (2006) 026.
- [21] PGS4 is a parametrized detector simulation. We use release 120611 in the CMS configuration (<http://www.physics.ucdavis.edu/~conway/research/software/pgs/pgs4-general.htm>).
- [22] M.L. Mangano, M. Moretti, F. Piccinini, M. Treccani, J. High Energy Phys. 01 (2007) 013.
- [23] U. Ellwanger, J.F. Gunion, C. Hugonie, J. High Energy Phys. 0502 (2005) 066;
U. Ellwanger, C. Hugonie, Comput. Phys. Commun. 175 (2006) 290;
G. Belanger, F. Boudjema, C. Hugonie, A. Pukhov, A. Semenov, J. Cosmol. Astropart. Phys. 0509 (2005) 001;
U. Ellwanger, C. Hugonie, Comput. Phys. Commun. 177 (2007) 399;
D. Das, U. Ellwanger, A.M. Teixeira, Comput. Phys. Commun. 183 (2012) 774;
M. Muhlleitner, A. Djouadi, Y. Mambrini, Comput. Phys. Commun. 168 (2005) 46.
- [24] W. Beenakker, R. Hopker, M. Spira, PROSPINO: A Program for the production of supersymmetric particles in next-to-leading order QCD, arXiv:hep-ph/9611232.
- [25] V. Khachatryan, et al., CMS Collaboration, Eur. Phys. J. C 74 (2014) 3036.
- [26] G. Aad, et al., ATLAS Collaboration, J. High Energy Phys. 04 (2014) 169;
G. Aad, et al., ATLAS Collaboration, J. High Energy Phys. 05 (2014) 071.
- [27] B. Dutta, T. Ghosh, A. Gurrola, W. Johns, T. Kamon, P. Sheldon, K. Sinha, K. Wang, et al., Phys. Rev. D 91 (2015) 055025;
Z. Han, Y. Liu, arXiv:1412.0618 [hep-ph];
A. Barr, J. Scoville, J. High Energy Phys. 04 (2015) 147.
- [28] J. Eckel, M.J. Ramsey-Musolf, W. Shepherd, S. Su, J. High Energy Phys. 11 (2014) 117.